The Rich Physics under Bosonic Double-Well Model

Tristan.W

December 30, 2025

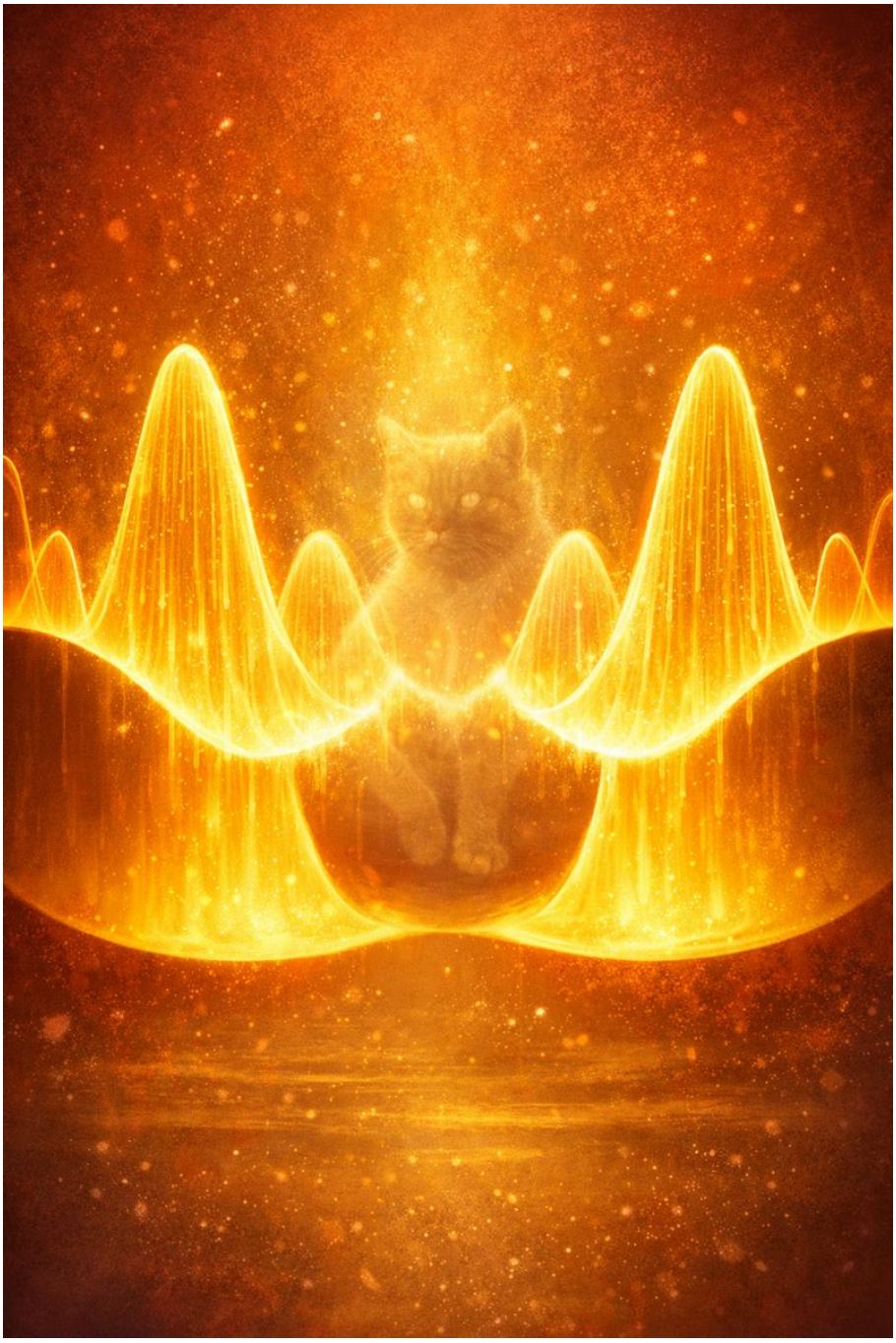

Contents

1 Two-Mode Double-Well Model: From Microscopic Hamiltonian to a Minimal Many-Body Problem

1.1 Two-mode truncation and single-particle structure

We consider interacting bosons in a symmetric double-well potential. Let $\psi_1(\boldsymbol{r})$ and $\psi_2(\boldsymbol{r})$ denote the lowest localized single-particle orbitals in the left and right well, respectively. The *two-mode approximation* assumes that all relevant dynamics takes place in the subspace spanned by these two orbitals, i.e. excited levels in each well are neglected.

This approximation is justified when (i) the barrier is sufficiently high such that tunneling between ψ_1 and ψ_2 is much weaker than the intrawell level spacing, and (ii) the typical interaction energy scale is also much smaller than the level spacing so that interactions do not significantly populate excited orbitals. Although these inequalities are not always strictly satisfied in experiments, the model is a useful minimal setting to expose the physics of phase coherence, number fluctuations, and measurement.

For a symmetric double well, the single-particle Hamiltonian is invariant under parity $x \leftrightarrow -x$. The symmetric and antisymmetric single-particle eigenstates are

$$\psi_g(\boldsymbol{r}) = \frac{1}{\sqrt{2}}\Big(\psi_1(\boldsymbol{r}) + \psi_2(\boldsymbol{r})\Big), \qquad \psi_e(\boldsymbol{r}) = \frac{1}{\sqrt{2}}\Big(\psi_1(\boldsymbol{r}) - \psi_2(\boldsymbol{r})\Big). \tag{1}$$

For a real single-particle Hamiltonian, the ground state can be chosen real and nodeless; hence ψ_g is the ground state.

1.2 Second quantization and derivation of the two-site Bose–Hubbard Hamiltonian

We start from the standard microscopic Hamiltonian for bosons with contact interaction (contact term)

$$\hat{H} = \int d^3r\, \hat{\Psi}^\dagger(\boldsymbol{r})\left(-\frac{\hbar^2\nabla^2}{2m} + V(\boldsymbol{r})\right)\hat{\Psi}(\boldsymbol{r}) + \frac{g}{2}\int d^3r\, \hat{\Psi}^\dagger(\boldsymbol{r})\hat{\Psi}^\dagger(\boldsymbol{r})\hat{\Psi}(\boldsymbol{r})\hat{\Psi}(\boldsymbol{r}), \tag{2}$$

where $\hat{\Psi}(\boldsymbol{r})$ is the bosonic field operator, m is the mass, $V(\boldsymbol{r})$ is the double-well potential, and g is the s-wave contact coupling (in 3D, $g = 4\pi\hbar^2 a_s/m$ in the usual dilute-gas setting).

In the two-mode approximation we expand

$$\hat{\Psi}(\boldsymbol{r}) = \psi_1(\boldsymbol{r})\hat{a}_1 + \psi_2(\boldsymbol{r})\hat{a}_2, \tag{3}$$

where $\hat{a}_i$ annihilates a boson in orbital ψ_i, and $[\hat{a}_i, \hat{a}_j^\dagger] = \delta_{ij}$. We also define number operators $\hat{n}_i = \hat{a}_i^\dagger\hat{a}_i$ and total number $\hat{N} = \hat{n}_1 + \hat{n}_2$.

Single-particle term and tunneling amplitude. Substituting the expansion into the single-particle part yields

$$\hat{H}_0 = \sum_{i,j=1}^{2} h_{ij}\,\hat{a}_i^\dagger\hat{a}_j, \qquad h_{ij} = \int d^3r\, \psi_i^*(\boldsymbol{r})\left(-\frac{\hbar^2\nabla^2}{2m} + V(\boldsymbol{r})\right)\psi_j(\boldsymbol{r}). \tag{4}$$

In a symmetric double well one typically has $h_{11} = h_{22} \equiv \epsilon_0$, and the off-diagonal matrix element $h_{12} = h_{21}$ gives tunneling. Writing

$$h_{12} = h_{21} \equiv -J, \tag{5}$$

we obtain (up to an additive constant $\epsilon_0\hat{N}$, which can be dropped since $\hat{N}$ is conserved)

$$\hat{H}_0 = -J\left(\hat{a}_1^\dagger\hat{a}_2 + \hat{a}_2^\dagger\hat{a}_1\right). \tag{6}$$

Interaction term and the origin of $\hat{n}(\hat{n}-1)$. The interaction term is

$$\hat{H}_{\rm int} = \frac{g}{2}\int d^3r\, \hat{\Psi}^\dagger(\boldsymbol{r})\hat{\Psi}^\dagger(\boldsymbol{r})\hat{\Psi}(\boldsymbol{r})\hat{\Psi}(\boldsymbol{r}). \tag{7}$$

Substituting the two-mode expansion produces quartic operator terms $\hat{a}_i^\dagger\hat{a}_j^\dagger\hat{a}_k\hat{a}_\ell$ multiplied by overlap integrals

$$U_{ijkl} \equiv g\int d^3r\, \psi_i^*(\boldsymbol{r})\psi_j^*(\boldsymbol{r})\psi_k(\boldsymbol{r})\psi_\ell(\boldsymbol{r}). \tag{8}$$

In the large-barrier regime, ψ_1 and ψ_2 have small spatial overlap. The dominant interaction terms are then the on-site terms U_{1111} and U_{2222}, while interwell interaction terms (such as U_{1122}, etc.) are parametrically smaller and are neglected in the simplest model. Defining

$$U \equiv g\int d^3r\, |\psi_1(\boldsymbol{r})|^4 \simeq g\int d^3r\, |\psi_2(\boldsymbol{r})|^4, \tag{9}$$

we get

$$\hat{H}_{\rm int} \simeq \frac{U}{2}\left(\hat{a}_1^\dagger\hat{a}_1^\dagger\hat{a}_1\hat{a}_1 + \hat{a}_2^\dagger\hat{a}_2^\dagger\hat{a}_2\hat{a}_2\right). \tag{10}$$

We now show explicitly why $\hat{a}^\dagger\hat{a}^\dagger\hat{a}\hat{a} = \hat{n}(\hat{n}-1)$. Let $\hat{n} = \hat{a}^\dagger\hat{a}$. Using $[\hat{a}, \hat{a}^\dagger] = 1$, we have

$$\hat{n}^2 = (\hat{a}^\dagger\hat{a})(\hat{a}^\dagger\hat{a}) = \hat{a}^\dagger(\hat{a}\hat{a}^\dagger)\hat{a} = \hat{a}^\dagger(\hat{a}^\dagger\hat{a}+1)\hat{a} = \hat{a}^\dagger\hat{a}^\dagger\hat{a}\hat{a} + \hat{a}^\dagger\hat{a}. \tag{11}$$

Therefore,

$$\hat{a}^\dagger\hat{a}^\dagger\hat{a}\hat{a} = \hat{n}^2 - \hat{n} = \hat{n}(\hat{n}-1). \tag{12}$$

Physically, $\hat{n}(\hat{n}-1)/2$ counts the number of unordered pairs among n identical bosons occupying the same mode, which is precisely what a local two-body contact interaction measures.

Combining $\hat{H}_0$ and $\hat{H}_{\rm int}$, we obtain the two-site Bose–Hubbard Hamiltonian

$$\hat{H} = -J\left(\hat{a}_1^\dagger\hat{a}_2 + \hat{a}_2^\dagger\hat{a}_1\right) + \frac{U}{2}\left[\hat{n}_1(\hat{n}_1-1) + \hat{n}_2(\hat{n}_2-1)\right]. \tag{13}$$

Throughout we take $\hbar$ explicit and assume fixed total particle number N (i.e. we work in a fixed-N sector).

The two-mode double-well Bose–Hubbard model is a minimal many-body system whose only low-energy collective degrees of freedom are the **relative number imbalance** $\Delta\hat{N} = \hat{n}_1 - \hat{n}_2$ and the **relative phase** θ between the two modes; tunneling J favors phase coherence, while interaction U favors number locking.

2 Mean-Field Description and the Energy Functional

2.1 What the mean-field ansatz means: a condensate as a macroscopically occupied mode

A mean-field ansatz in this context asserts that all N bosons occupy the same single-particle orbital, which is itself a coherent superposition of the two localized modes. Concretely, define a normalized single-particle creation operator

$$\hat{b}^\dagger \equiv c_1\hat{a}_1^\dagger + c_2\hat{a}_2^\dagger, \qquad |c_1|^2 + |c_2|^2 = 1. \tag{14}$$

The corresponding N-boson condensate state is

$$|\Psi_{\rm MF}(c_1, c_2)\rangle \equiv \frac{1}{\sqrt{N!}}(\hat{b}^\dagger)^N|0\rangle. \tag{15}$$

This is the precise meaning of "all bosons are condensed in the same single-particle state" within a fixed-N Hilbert space.

A convenient parametrization is

$$c_1 = \cos\frac{\alpha}{2}\, e^{-i\theta/2}, \qquad c_2 = \sin\frac{\alpha}{2}\, e^{+i\theta/2}, \tag{16}$$

where θ is the relative phase and α controls the population imbalance. The mean-field state becomes

$$|\Psi_{\mathrm{MF}}\rangle = \frac{1}{\sqrt{N!}}\left(\cos\frac{\alpha}{2}e^{-i\theta/2}\hat{a}_1^\dagger + \sin\frac{\alpha}{2}e^{i\theta/2}\hat{a}_2^\dagger\right)^N |0\rangle. \tag{17}$$

We emphasize that in a fixed-N setting this is a perfectly well-defined many-body state (not a symmetry-breaking coherent state of $\hat{a}_i$ themselves); it is simply an SU(2) coherent state (a fully polarized spin state in the Schwinger boson representation).

Schwinger boson representation and SU(2) coherent states: why "spin" appears in a two-mode Bose system

In a two-mode problem, each boson carries a *mode index* (left/right, or 1/2), which is mathematically a two-level degree of freedom. Even though the bosons do *not* have an intrinsic physical spin here, the two-mode algebra naturally generates an $\mathfrak{su}(2)$ structure. The **Schwinger boson representation** is precisely the standard way to realize angular-momentum operators using two bosonic modes.

(1) Definition: $\mathfrak{su}(2)$ generators as bilinears of two bosons. Given two bosonic modes $\hat{a}_1, \hat{a}_2$ with $[\hat{a}_i, \hat{a}_j^\dagger] = \delta_{ij}$, define

$$\hat{S}_x = \frac{1}{2}\left(\hat{a}_1^\dagger\hat{a}_2 + \hat{a}_2^\dagger\hat{a}_1\right), \qquad \hat{S}_y = \frac{1}{2i}\left(\hat{a}_1^\dagger\hat{a}_2 - \hat{a}_2^\dagger\hat{a}_1\right), \qquad \hat{S}_z = \frac{1}{2}\left(\hat{n}_1 - \hat{n}_2\right), \tag{18}$$

with $\hat{n}_i = \hat{a}_i^\dagger\hat{a}_i$, and $\hat{N} = \hat{n}_1 + \hat{n}_2$. One can verify directly that

$$[\hat{S}_\mu, \hat{S}_\nu] = i\,\epsilon_{\mu\nu\lambda}\hat{S}_\lambda, \tag{19}$$

so $\hat{\mathbf{S}} = (\hat{S}_x, \hat{S}_y, \hat{S}_z)$ forms an $\mathfrak{su}(2)$ algebra. Moreover, the Casimir takes a fixed value in a fixed-N sector:

$$\hat{\mathbf{S}}^2 = \hat{S}_x^2 + \hat{S}_y^2 + \hat{S}_z^2 = \frac{\hat{N}}{2}\left(\frac{\hat{N}}{2} + 1\right), \tag{20}$$

so if the total particle number is fixed to N, then the system lives in a single irreducible spin representation with

$$S = \frac{N}{2}. \tag{21}$$

In this sense, the $\hat{S}$'s describe a **collective (pseudo-)spin** of length $N/2$: it encodes how the N bosons are distributed between the two modes, not any intrinsic spin carried by each atom.

(2) Why introduce this representation? There are two key reasons.

First, it makes the physical degrees of freedom explicit: $\hat{S}_z = \Delta\hat{N}/2$ is the **number imbalance** operator, while $\hat{S}_x, \hat{S}_y$ encode **phase coherence** through off-diagonal correlators such as $\hat{a}_1^\dagger\hat{a}_2$. In particular,

$$\hat{a}_1^\dagger\hat{a}_2 = \hat{S}_x + i\hat{S}_y. \tag{22}$$

Second, it turns the two-site Bose–Hubbard Hamiltonian into a compact "spin" Hamiltonian (up to an N-dependent constant):

$$\hat{H} = -J\left(\hat{a}_1^\dagger\hat{a}_2 + \hat{a}_2^\dagger\hat{a}_1\right) + \frac{U}{2}\left[\hat{n}_1(\hat{n}_1 - 1) + \hat{n}_2(\hat{n}_2 - 1)\right] = -2J\,\hat{S}_x + U\,\hat{S}_z^2 + \text{const.} \tag{23}$$

This immediately reveals the competition: tunneling tries to align the collective spin along $+x$ (maximal coherence), while interaction tries to localize S_z (number squeezing). Many results (Josephson dynamics, self-trapping, cat states for $U < 0$) can then be interpreted as familiar "large-spin" physics.

(3) What is an SU(2) **coherent state in this language?** Fix N so that $S = N/2$. The "fully polarized" (highest-weight) state is

$$|S, S\rangle \equiv \frac{(\hat{a}_1^\dagger)^N}{\sqrt{N!}}|0\rangle, \tag{24}$$

i.e. all bosons occupy mode 1. An SU(2) coherent state is obtained by an SU(2) rotation of this polarized state:

$$|\alpha, \theta\rangle \equiv e^{-i\theta\hat{S}_z} e^{-i\alpha\hat{S}_y} |S, S\rangle. \tag{25}$$

Equivalently (and this is exactly your mean-field ansatz), it can be written as a condensate of a rotated single-particle creation operator

$$|\alpha, \theta\rangle = \frac{1}{\sqrt{N!}} \left(\cos\frac{\alpha}{2} e^{-i\theta/2} \hat{a}_1^\dagger + \sin\frac{\alpha}{2} e^{i\theta/2} \hat{a}_2^\dagger \right)^N |0\rangle. \tag{26}$$

This is why the fixed-N mean-field state is naturally called an SU(2) coherent state: it is the most "classical" state of a large collective spin (it minimizes quantum fluctuations transverse to its polarization direction on the Bloch sphere).

(4) The meaning of "spin" variables and their geometric interpretation. The angles (α, θ) are precisely spherical coordinates of a unit vector $\boldsymbol{n}$ on the Bloch sphere:

$$\boldsymbol{n} = (\sin\alpha\cos\theta,\ \sin\alpha\sin\theta,\ \cos\alpha). \tag{27}$$

In the coherent state $|\alpha, \theta\rangle$, the collective spin has a classical expectation value

$$\langle \hat{\boldsymbol{S}} \rangle = S\,\boldsymbol{n} = \frac{N}{2}\boldsymbol{n}, \tag{28}$$

so explicitly

$$\langle \hat{S}_z \rangle = \frac{1}{2}\langle \Delta\hat{N} \rangle = \frac{N}{2}\cos\alpha, \qquad \langle \hat{a}_1^\dagger \hat{a}_2 \rangle = \langle \hat{S}_x + i\hat{S}_y \rangle = \frac{N}{2}\sin\alpha\, e^{i\theta}. \tag{29}$$

Hence α controls the population imbalance (through $\cos\alpha$), while θ is the relative phase associated with first-order coherence (through the phase of $\langle \hat{a}_1^\dagger \hat{a}_2 \rangle$). In this sense, "spin" is simply a compact encoding of the two collective degrees of freedom: imbalance and relative phase.

2.2 Expectation values in the mean-field state and derivation of the energy functional

We now compute the expectation values that enter $\mathcal{E} = \langle \Psi_{\mathrm{MF}} | \hat{H} | \Psi_{\mathrm{MF}} \rangle$. The key structural fact is that $|\Psi_{\mathrm{MF}}\rangle$ has all particles in the $\hat{b}$ mode, so correlation functions reduce to combinatorics controlled by (c_1, c_2).

One-body correlators $\langle \hat{a}_i^\dagger \hat{a}_j \rangle$. We first show

$$\langle \hat{a}_i^\dagger \hat{a}_j \rangle = N c_i^* c_j. \tag{30}$$

To prove this, choose an orthonormal complementary mode

$$\hat{d}^\dagger \equiv -c_2^* \hat{a}_1^\dagger + c_1^* \hat{a}_2^\dagger, \qquad [\hat{b}, \hat{b}^\dagger] = [\hat{d}, \hat{d}^\dagger] = 1, \qquad [\hat{b}, \hat{d}^\dagger] = 0, \tag{31}$$

so that the transformation between $(\hat{a}_1, \hat{a}_2)$ and $(\hat{b}, \hat{d})$ is unitary:

$$\hat{a}_1 = c_1 \hat{b} - c_2 \hat{d}, \qquad \hat{a}_2 = c_2 \hat{b} + c_1 \hat{d}, \tag{32}$$

where for notational simplicity we understand c_1, c_2 in the above as the same numbers entering $\hat{b}^\dagger$ (the precise complex conjugations are fixed by the unitarity; the final correlators depend only on $c_i^* c_j$).

Since $|\Psi_{\rm MF}\rangle \propto (\hat{b}^\dagger)^N |0\rangle$ has zero occupation in the $\hat{d}$ mode, any operator containing an unmatched $\hat{d}$ or $\hat{d}^\dagger$ has vanishing expectation. Using $\hat{b}|\Psi_{\rm MF}\rangle = \sqrt{N}\,|\Psi_{\rm MF}^{(N-1)}\rangle$ and $\langle \hat{b}^\dagger \hat{b}\rangle = N$, we obtain

$$\langle \hat{a}_i^\dagger \hat{a}_j \rangle = \langle (c_i^* \hat{b}^\dagger + \cdots)(c_j \hat{b} + \cdots)\rangle = c_i^* c_j \langle \hat{b}^\dagger \hat{b}\rangle = N c_i^* c_j, \tag{33}$$

as claimed.

With the parametrization (α, θ),

$$\langle \hat{n}_1 \rangle = N \cos^2 \frac{\alpha}{2}, \qquad \langle \hat{n}_2 \rangle = N \sin^2 \frac{\alpha}{2}, \qquad \langle \hat{a}_1^\dagger \hat{a}_2 \rangle = N \sin \frac{\alpha}{2} \cos \frac{\alpha}{2}\, e^{i\theta} = \frac{N}{2} \sin \alpha\, e^{i\theta}. \tag{34}$$

The number imbalance satisfies

$$\langle \Delta \hat{N} \rangle = \langle \hat{n}_1 - \hat{n}_2 \rangle = N \cos \alpha. \tag{35}$$

Two-body on-site correlators $\langle \hat{n}_i(\hat{n}_i - 1)\rangle$. We also need $\langle \hat{a}_i^\dagger \hat{a}_i^\dagger \hat{a}_i \hat{a}_i \rangle$. Using $\hat{a}_i = c_i \hat{b}$+(terms with $\hat{d}$) and the same "$\hat{d}$-vacuum" argument, we get

$$\langle \hat{a}_i^\dagger \hat{a}_i^\dagger \hat{a}_i \hat{a}_i \rangle = |c_i|^4 \langle \hat{b}^\dagger \hat{b}^\dagger \hat{b} \hat{b} \rangle. \tag{36}$$

Now

$$\hat{b}^\dagger \hat{b}^\dagger \hat{b} \hat{b} = \hat{N}_b (\hat{N}_b - 1), \qquad \hat{N}_b \equiv \hat{b}^\dagger \hat{b}. \tag{37}$$

Since $|\Psi_{\rm MF}\rangle$ is an $\hat{N}_b = N$ eigenstate, we have

$$\langle \hat{b}^\dagger \hat{b}^\dagger \hat{b} \hat{b} \rangle = N(N-1). \tag{38}$$

Therefore,

$$\langle \hat{n}_i(\hat{n}_i - 1)\rangle = \langle \hat{a}_i^\dagger \hat{a}_i^\dagger \hat{a}_i \hat{a}_i \rangle = N(N-1)|c_i|^4. \tag{39}$$

In terms of α,

$$|c_1|^4 = \cos^4 \frac{\alpha}{2}, \qquad |c_2|^4 = \sin^4 \frac{\alpha}{2}, \qquad \cos^4 \frac{\alpha}{2} + \sin^4 \frac{\alpha}{2} = \frac{1}{2}\left(1 + \cos^2 \alpha\right). \tag{40}$$

Energy functional. We now compute $\mathcal{E} = \langle \hat{H} \rangle$.

For the tunneling term,

$$\langle \hat{H}_0 \rangle = -J\left(\langle \hat{a}_1^\dagger \hat{a}_2 \rangle + \langle \hat{a}_2^\dagger \hat{a}_1 \rangle\right) = -2J\,\mathrm{Re}\,\langle \hat{a}_1^\dagger \hat{a}_2 \rangle = -JN \sin \alpha \cos \theta. \tag{41}$$

For the interaction term,

$$\langle \hat{H}_{\rm int} \rangle = \frac{U}{2} \sum_{i=1}^{2} \langle \hat{n}_i(\hat{n}_i - 1)\rangle = \frac{U}{2} N(N-1)\left(|c_1|^4 + |c_2|^4\right) = \frac{U}{4} N(N-1)\left(1 + \cos^2 \alpha\right). \tag{42}$$

Thus

$$\mathcal{E}(\alpha,\theta) = -JN\sin\alpha\cos\theta + \frac{U}{4}N(N-1)\left(1+\cos^2\alpha\right). \tag{43}$$

Up to an α-independent constant $\frac{U}{4}N(N-1)$, one often writes

$$\mathcal{E}(\alpha,\theta) = -JN\sin\alpha\cos\theta + \frac{U}{4}N(N-1)\cos^2\alpha. \tag{44}$$

In the large-N mean-field scaling, $N(N-1) \simeq N^2$, matching the form commonly quoted in the literature.

2.3 Mean-field ground states for repulsive and attractive interactions

We now minimize $\mathcal{E}(\alpha,\theta)$ at fixed N, focusing on its dependence on α and θ.

Repulsive interaction $U > 0$. Since $J > 0$, the tunneling term is minimized by $\cos\theta = 1$, i.e. $\theta = 0$ modulo 2π. With $\theta = 0$, the α-dependent part is

$$\mathcal{E}(\alpha,0) = -JN\sin\alpha + \frac{U}{4}N(N-1)\cos^2\alpha + \text{const.} \tag{45}$$

For repulsive $U > 0$, both the tunneling term (which favors maximal $\sin\alpha$) and the interaction term (which favors $\cos^2\alpha$ small) select $\alpha = \pi/2$. Hence the mean-field ground state is

$$|\Psi_{\mathrm{MF}}\rangle = \frac{1}{\sqrt{N!}}\left(\frac{\hat{a}_1^\dagger + \hat{a}_2^\dagger}{\sqrt{2}}\right)^N |0\rangle, \tag{46}$$

i.e. all particles occupy the symmetric single-particle orbital ψ_g, with balanced populations and a well-defined relative phase.

Attractive interaction $U < 0$ and the appearance of two degenerate minima. For $U < 0$, the interaction term favors large $|\cos\alpha|$, i.e. macroscopic population imbalance. Setting again $\theta = 0$ to minimize tunneling, the stationarity condition $\partial_\alpha \mathcal{E}(\alpha,0) = 0$ yields

$$-JN\cos\alpha - \frac{U}{2}N(N-1)\sin\alpha\cos\alpha = 0. \tag{47}$$

Assuming $\cos\alpha \neq 0$, we get

$$\sin\alpha = \frac{2J}{|U|(N-1)}. \tag{48}$$

Thus if $|U|(N-1) > 2J$ there are two solutions

$$\alpha_0 = \arcsin\left(\frac{2J}{|U|(N-1)}\right), \qquad \pi - \alpha_0, \tag{49}$$

corresponding to opposite signs of $\cos\alpha$ (i.e. opposite imbalances). In the strong-attraction limit $U \to -\infty$, $\alpha_0 \to 0$ and $\pi - \alpha_0 \to \pi$, so the mean-field minima approach states with all bosons in one well, schematically $\hat{a}_1^{\dagger N}|0\rangle$ or $\hat{a}_2^{\dagger N}|0\rangle$. These states break the left-right exchange Z_2 symmetry at the mean-field level.

3 Exact Quantum Solution in the Fock Basis and the Discrete Schrödinger Equation

3.1 Fixed-N Hilbert space, spin mapping, and matrix elements

Because $\hat{N}$ is conserved, we work in the N-particle sector spanned by Fock states $|N_1, N_2\rangle$ with $N_1 + N_2 = N$. It is convenient to parameterize

$$N_1 = \frac{N}{2} + l, \qquad N_2 = \frac{N}{2} - l, \qquad l = -\frac{N}{2}, -\frac{N}{2} + 1, \ldots, \frac{N}{2}. \tag{50}$$

A general state is

$$|\Psi\rangle = \sum_l \Psi_l \left| \frac{N}{2} + l, \frac{N}{2} - l \right\rangle. \tag{51}$$

It is also useful to introduce the Schwinger boson (collective spin) operators

$$\hat{S}_x = \frac{1}{2}(\hat{a}_1^\dagger \hat{a}_2 + \hat{a}_2^\dagger \hat{a}_1), \qquad \hat{S}_y = \frac{1}{2i}(\hat{a}_1^\dagger \hat{a}_2 - \hat{a}_2^\dagger \hat{a}_1), \qquad \hat{S}_z = \frac{1}{2}(\hat{n}_1 - \hat{n}_2) = \frac{1}{2}\Delta\hat{N}. \tag{52}$$

In the fixed-N sector, the total spin is $\hat{\mathbf{S}}^2 = S(S+1)$ with $S = N/2$, and the basis $|l\rangle \equiv |N/2+l, N/2-l\rangle$ is the $\hat{S}_z$ eigenbasis, $\hat{S}_z|l\rangle = l|l\rangle$.

In this language, up to an N-dependent constant, the Hamiltonian becomes

$$\hat{H} = -2J\,\hat{S}_x + U\,\hat{S}_z^2 + \text{const.} \tag{53}$$

This form already indicates that tunneling tries to align the spin along x (phase coherence), while interaction tries to pin S_z (number imbalance).

3.2 Derivation of the discrete Schrödinger equation (recurrence relation for Ψ_l)

We now derive the recurrence relation by acting with $\hat{H}$ on the basis states.

Tunneling matrix elements. Using $\hat{a}|n\rangle = \sqrt{n}|n-1\rangle$ and $\hat{a}^\dagger|n\rangle = \sqrt{n+1}|n+1\rangle$,

$$\hat{a}_1^\dagger \hat{a}_2 \,|N_1, N_2\rangle = \sqrt{(N_1+1)N_2}\,|N_1+1, N_2-1\rangle, \tag{54}$$

$$\hat{a}_2^\dagger \hat{a}_1 \,|N_1, N_2\rangle = \sqrt{(N_2+1)N_1}\,|N_1-1, N_2+1\rangle. \tag{55}$$

In terms of l,

$$\hat{a}_1^\dagger \hat{a}_2 \,|l\rangle = \sqrt{\left(\frac{N}{2}+l+1\right)\left(\frac{N}{2}-l\right)}\,|l+1\rangle, \tag{56}$$

$$\hat{a}_2^\dagger \hat{a}_1 \,|l\rangle = \sqrt{\left(\frac{N}{2}-l+1\right)\left(\frac{N}{2}+l\right)}\,|l-1\rangle. \tag{57}$$

Therefore,

$$-J(\hat{a}_1^\dagger \hat{a}_2 + \hat{a}_2^\dagger \hat{a}_1)|\Psi\rangle = -\sum_l \left(K_{l+1}\Psi_{l+1} + K_l \Psi_{l-1}\right)|l\rangle, \tag{58}$$

where we defined the positive hopping coefficients

$$K_l \equiv J\sqrt{\left(\frac{N}{2}+l\right)\left(\frac{N}{2}-l+1\right)}. \tag{59}$$

Interaction energy in the $|l\rangle$ basis. The interaction term is diagonal in $|N_1, N_2\rangle$:

$$\frac{U}{2}\left[\hat{n}_1(\hat{n}_1-1)+\hat{n}_2(\hat{n}_2-1)\right]|N_1,N_2\rangle = \frac{U}{2}\left[N_1(N_1-1)+N_2(N_2-1)\right]|N_1,N_2\rangle. \tag{60}$$

Substitute $N_{1,2} = N/2 \pm l$:

$$N_1(N_1-1)+N_2(N_2-1) = \left(\frac{N}{2}+l\right)\left(\frac{N}{2}+l-1\right)+\left(\frac{N}{2}-l\right)\left(\frac{N}{2}-l-1\right). \tag{61}$$

Expanding,

$$N_1(N_1-1)+N_2(N_2-1) = \frac{N(N-2)}{2}+2l^2. \tag{62}$$

Thus,

$$\hat{H}_{\text{int}}|l\rangle = \left[Ul^2+\frac{U}{4}N(N-2)\right]|l\rangle. \tag{63}$$

The constant shift $\frac{U}{4}N(N-2)$ can be absorbed into the eigenenergy.

The recurrence relation. Projecting the eigenvalue equation $\hat{H}|\Psi\rangle = E|\Psi\rangle$ onto $\langle l|$ gives the discrete Schrödinger equation

$$E'\Psi_l = -K_{l+1}\Psi_{l+1} - K_l\Psi_{l-1} + Ul^2\Psi_l, \tag{64}$$

where $E' \equiv E - \frac{U}{4}N(N-2)$.

Projecting the fixed-N two-site Bose–Hubbard Hamiltonian onto the number-imbalance basis $|l\rangle$ yields a **discrete Schrödinger equation** (64) in the "coordinate" l, with tunneling providing nearest-neighbor hopping in l and interaction providing an effective potential Ul^2.

4 Number Fluctuations: Gaussian Wavefunctions from $U = 0$ to Strong Repulsion

4.1 Noninteracting limit $U = 0$: binomial coefficients and the Gaussian approximation

For $U = 0$, the ground state places all bosons in the symmetric mode $\hat{b}_g^\dagger = (\hat{a}_1^\dagger + \hat{a}_2^\dagger)/\sqrt{2}$:

$$|\Psi\rangle = \frac{1}{\sqrt{N!}}\left(\frac{\hat{a}_1^\dagger+\hat{a}_2^\dagger}{\sqrt{2}}\right)^N|0\rangle. \tag{65}$$

Detailed Derivation of the $U = 0$ Ground State

For $U = 0$, the Hamiltonian contains only the tunneling term

$$\hat{H}_0 = -J(\hat{a}_1^\dagger\hat{a}_2+\hat{a}_2^\dagger\hat{a}_1), \qquad (J>0). \tag{66}$$

To identify the ground state, it is convenient to first diagonalize $\hat{H}_0$ in the single-particle Hilbert space spanned by the localized states $\{|1\rangle, |2\rangle\}$. In this basis, $\hat{H}_0$ is represented by the 2×2 matrix

$$H_0^{(1)} = \begin{pmatrix} 0 & -J \\ -J & 0 \end{pmatrix}. \tag{67}$$

Solving the eigenvalue problem $H_0^{(1)} v = \varepsilon\, v$, one immediately finds two orthonormal eigenvectors

$$v_g = \frac{1}{\sqrt{2}}\begin{pmatrix}1\\1\end{pmatrix}, \qquad v_e = \frac{1}{\sqrt{2}}\begin{pmatrix}1\\-1\end{pmatrix}, \tag{68}$$

with eigenvalues

$$\varepsilon_g = -J, \qquad \varepsilon_e = +J. \tag{69}$$

Equivalently, in second quantization we introduce the symmetric/antisymmetric mode operators

$$\hat{b}_g^\dagger = \frac{\hat{a}_1^\dagger + \hat{a}_2^\dagger}{\sqrt{2}}, \qquad \hat{b}_e^\dagger = \frac{\hat{a}_1^\dagger - \hat{a}_2^\dagger}{\sqrt{2}}, \tag{70}$$

under which the tunneling term becomes diagonal:

$$\hat{a}_1^\dagger \hat{a}_2 + \hat{a}_2^\dagger \hat{a}_1 = \hat{b}_g^\dagger \hat{b}_g - \hat{b}_e^\dagger \hat{b}_e, \qquad \Rightarrow \qquad \hat{H}_0 = -J(\hat{n}_g - \hat{n}_e), \tag{71}$$

where $\hat{n}_g = \hat{b}_g^\dagger \hat{b}_g$ and $\hat{n}_e = \hat{b}_e^\dagger \hat{b}_e$. In a fixed-$N$ sector, $\hat{n}_g + \hat{n}_e = N$, so the energy of a Fock configuration $|n_g, n_e\rangle$ is

$$E(n_g, n_e) = -J(n_g - n_e) = -JN + 2J\, n_e. \tag{72}$$

Since $J > 0$, the energy is minimized uniquely by $n_e = 0$, i.e. all bosons occupy the symmetric orbital. Therefore the many-body ground state is

$$|\Psi\rangle = \frac{1}{\sqrt{N!}} \left(\hat{b}_g^\dagger\right)^N |0\rangle = \frac{1}{\sqrt{N!}} \left(\frac{\hat{a}_1^\dagger + \hat{a}_2^\dagger}{\sqrt{2}}\right)^N |0\rangle. \tag{73}$$

Expanding with the binomial theorem,

$$\left(\hat{a}_1^\dagger + \hat{a}_2^\dagger\right)^N = \sum_{N_1=0}^{N} \binom{N}{N_1} (\hat{a}_1^\dagger)^{N_1} (\hat{a}_2^\dagger)^{N-N_1}. \tag{74}$$

Thus in the normalized Fock basis,

$$|\Psi\rangle = \sum_{N_1=0}^{N} \Psi_{N_1} |N_1, N - N_1\rangle, \qquad \Psi_{N_1} = \sqrt{\frac{N!}{2^N N_1!(N-N_1)!}}. \tag{75}$$

With $N_1 = N/2 + l$,

$$\Psi_l = \sqrt{\frac{N!}{2^N \left(\frac{N}{2}+l\right)! \left(\frac{N}{2}-l\right)!}}. \tag{76}$$

We now derive the Gaussian approximation for large N and $|l| \ll N$. Using Stirling's approximation (with the level needed here)

$$\log n! = n \log n - n + \frac{1}{2}\log(2\pi n) + O\left(\frac{1}{n}\right), \tag{77}$$

we consider

$$\log |\Psi_l|^2 = \log N! - N \log 2 - \log\left(\frac{N}{2}+l\right)! - \log\left(\frac{N}{2}-l\right)!. \tag{78}$$

Expand around $l = 0$. Define $f(x) = \log x!$ and Taylor expand $f(N/2 \pm l)$ in l:

$$f\left(\frac{N}{2} \pm l\right) = f\left(\frac{N}{2}\right) \pm l f'\left(\frac{N}{2}\right) + \frac{l^2}{2} f''\left(\frac{N}{2}\right) + O\left(\frac{l^3}{N^2}\right). \tag{79}$$

The odd terms cancel when summing $f(N/2+l)+f(N/2-l)$. Using $f'(x) \simeq \log x$ and $f''(x) \simeq 1/x$ at large x, we obtain

$$f\left(\frac{N}{2}+l\right)+f\left(\frac{N}{2}-l\right) \simeq 2f\left(\frac{N}{2}\right)+\frac{l^2}{\frac{N}{2}}. \tag{80}$$

Hence

$$\log|\Psi_l|^2 \simeq \text{const} - \frac{2l^2}{N}, \tag{81}$$

so

$$\Psi_l \approx \frac{1}{(\pi N/4)^{1/4}}\, e^{-2l^2/N}. \tag{82}$$

The probability distribution $|\Psi_l|^2 \propto e^{-4l^2/N}$ has variance

$$\text{Var}(l) = \frac{N}{8}. \tag{83}$$

Since $\Delta N = 2l$, we find

$$\langle(\Delta\hat{N})^2\rangle = 4\,\text{Var}(l) = \frac{N}{2} \sim O(N), \tag{84}$$

which is the expected central-limit scaling for a binomial distribution.

4.2 Repulsive interaction and the harmonic-oscillator approximation in number space

For $U > 0$, Eq. (64) shows that the effective potential Ul^2 confines Ψ_l near $l = 0$. When the wavefunction is localized such that $|l| \ll N$ dominates, we may approximate

$$K_l = J\sqrt{\left(\frac{N}{2}+l\right)\left(\frac{N}{2}-l+1\right)} \simeq \frac{JN}{2} \equiv K, \tag{85}$$

treating K as a constant. Then Eq. (64) reduces to

$$E'\Psi_l \simeq -K(\Psi_{l+1}+\Psi_{l-1}) + Ul^2\Psi_l. \tag{86}$$

It is useful to rewrite the hopping term as a discrete Laplacian plus a constant:

$$\Psi_{l+1}+\Psi_{l-1} = 2\Psi_l + (\Psi_{l+1} - 2\Psi_l + \Psi_{l-1}), \tag{87}$$

so

$$(E'+2K)\Psi_l \simeq -K(\Psi_{l+1} - 2\Psi_l + \Psi_{l-1}) + Ul^2\Psi_l. \tag{88}$$

If Ψ_l varies slowly on the scale of $\Delta l = 1$, we take the continuum approximation

$$\Psi_{l+1} - 2\Psi_l + \Psi_{l-1} \approx \frac{d^2\Psi}{dl^2}, \tag{89}$$

obtaining an effective Schrödinger equation

$$\left[-K\frac{d^2}{dl^2} + Ul^2\right]\Psi(l) = \mathcal{E}\,\Psi(l), \tag{90}$$

where $\mathcal{E} = E' + 2K$ is a shifted energy.

Equation (90) is the stationary Schrödinger equation of a harmonic oscillator in the "coordinate" l, with an effective kinetic coefficient K and spring constant U. The ground-state wavefunction is Gaussian,

$$\Psi(l) \propto \exp\left(-\frac{l^2}{2\sigma_l^2}\right), \tag{91}$$

with width determined by balancing kinetic and potential energies. Substituting into (90) and matching coefficients gives

$$\sigma_l^2 \sim \sqrt{\frac{K}{U}} \sim \sqrt{\frac{JN}{U}}. \tag{92}$$

Therefore the number-imbalance fluctuation scales as

$$\langle (\Delta \hat{N})^2 \rangle \sim 4\,\sigma_l^2 \propto \sqrt{\frac{JN}{U}}, \tag{93}$$

showing strong suppression of number fluctuations as U increases.

In the extreme limit $JN/U \ll 1$, Ψ_l becomes sharply localized at $l = 0$, and the state approaches the Fock state

$$|\Psi\rangle \to \left|\frac{N}{2}, \frac{N}{2}\right\rangle = \frac{\hat{a}_1^{\dagger N/2} \hat{a}_2^{\dagger N/2}}{(N/2)!}|0\rangle, \tag{94}$$

which is an eigenstate of $\Delta \hat{N}$ with vanishing fluctuations.

5 Phase Coherence, Fragmentation, and the Number–Phase Complementarity

5.1 One-body density matrix and the definition of fragmentation

The one-body density matrix in the two-mode subspace is

$$\rho^{(1)} = \begin{pmatrix} \langle \hat{a}_1^\dagger \hat{a}_1 \rangle & \langle \hat{a}_1^\dagger \hat{a}_2 \rangle \\ \langle \hat{a}_2^\dagger \hat{a}_1 \rangle & \langle \hat{a}_2^\dagger \hat{a}_2 \rangle \end{pmatrix}. \tag{95}$$

A *simple condensate* (simple BEC) is characterized by a single eigenvalue of $\rho^{(1)}$ that scales as $O(N)$, with all other eigenvalues parametrically smaller. A *fragmented condensate* has two (or more) eigenvalues scaling as $O(N)$, indicating macroscopic occupation of multiple orthogonal single-particle modes.

For the noninteracting symmetric condensate,

$$\langle \hat{n}_1 \rangle = \langle \hat{n}_2 \rangle = \frac{N}{2}, \qquad \langle \hat{a}_1^\dagger \hat{a}_2 \rangle = \frac{N}{2}, \tag{96}$$

so

$$\rho^{(1)} = \frac{N}{2} \begin{pmatrix} 1 & 1 \\ 1 & 1 \end{pmatrix}, \tag{97}$$

whose eigenvalues are $(N, 0)$. This is a simple BEC.

In the strong-repulsion Fock limit $|N/2, N/2\rangle$, one has

$$\langle \hat{a}_1^\dagger \hat{a}_2 \rangle = 0, \qquad \langle \hat{n}_1 \rangle = \langle \hat{n}_2 \rangle = \frac{N}{2}, \tag{98}$$

hence

$$\rho^{(1)} = \frac{N}{2} \begin{pmatrix} 1 & 0 \\ 0 & 1 \end{pmatrix}, \tag{99}$$

whose eigenvalues are $(N/2, N/2)$, both macroscopic. This is a fragmented condensate.

5.2 Quadratic expansion near the repulsive mean-field minimum and phase fluctuations

To connect the exact-number picture to a phase-fluctuation picture, we revisit the mean-field energy landscape for $U > 0$, which is minimized at $\alpha = \pi/2$ and $\theta = 0$. Expand

$$\alpha = \frac{\pi}{2} + \delta\alpha, \qquad |\delta\alpha| \ll 1, \qquad |\theta| \ll 1. \tag{100}$$

Using

$$\sin\alpha = \sin\left(\frac{\pi}{2} + \delta\alpha\right) \approx 1 - \frac{\delta\alpha^2}{2}, \qquad \cos\alpha \approx -\delta\alpha, \qquad \cos\theta \approx 1 - \frac{\theta^2}{2}, \tag{101}$$

the mean-field energy (dropping constants) becomes

$$\mathcal{E} \approx \frac{JN}{2}\theta^2 + \frac{U}{4}N(N-1)\delta\alpha^2. \tag{102}$$

Since $\langle\Delta\hat{N}\rangle = N\cos\alpha \approx -N\delta\alpha$, we can rewrite this as

$$\mathcal{E} \approx \frac{JN}{2}\theta^2 + \frac{U}{4}\frac{N-1}{N}(\Delta N)^2 \approx \frac{JN}{2}\theta^2 + \frac{U}{4}(\Delta N)^2, \tag{103}$$

where the final approximation uses large N.

Equation (103) has the structure of a harmonic oscillator Hamiltonian if θ and ΔN are treated as conjugate variables. The precise definition of a Hermitian phase operator is subtle in finite-dimensional Hilbert spaces; however, in the large-N regime with small fluctuations, it is consistent and standard to treat θ as a continuous variable conjugate to ΔN, leading to an uncertainty relation of the schematic form

$$\sigma_{\Delta N}^2\,\sigma_\theta^2 \sim N, \tag{104}$$

capturing the complementarity: suppressing number fluctuations (number squeezing) increases phase fluctuations, and vice versa.

In the repulsive two-mode Bose–Hubbard model, increasing U/J continuously drives the system from a regime with a well-defined relative phase and large number fluctuations $\langle(\Delta\hat{N})^2\rangle \sim O(N)$ to a regime with strong number squeezing $\langle(\Delta\hat{N})^2\rangle \ll N$ and large phase fluctuations, culminating in a fragmented Fock-like state with vanishing first-order coherence $\langle\hat{a}_1^\dagger\hat{a}_2\rangle \to 0$.

6 Josephson Effects: Current Operator and Coupled Dynamics of ΔN and θ

In a bosonic double-well, the Josephson effect is the dynamical manifestation of *phase coherence* across a weak link. The key collective variables are the relative number imbalance $\Delta\hat{N} = \hat{n}_1 - \hat{n}_2$ and the relative phase θ between the two modes. In a coherent (single-condensate) regime, a nonzero θ can drive an interwell particle current even without an externally imposed bias, while interactions make the relative phase sensitive to the number imbalance. At the mean-field level, this intuition is captured by the energy functional $\mathcal{E}(\alpha, \theta)$ and leads to coupled equations of motion for ΔN and θ, closely analogous to a classical Josephson junction. In the quantum two-mode model, however, the most precise and conceptually clean route is to *define* the current operator through the Heisenberg equation for $\Delta\hat{N}$, which immediately clarifies which Hamiltonian term generates transport and how the number-phase coupled dynamics emerges.

6.1 Which "current term"? The current operator comes from the tunneling Hamiltonian

The only Hamiltonian term that transfers particles between wells is the tunneling term

$$\hat{H}_J \equiv -J(\hat{a}_1^\dagger \hat{a}_2 + \hat{a}_2^\dagger \hat{a}_1). \tag{105}$$

The interaction term depends only on $\hat{n}_1$ and $\hat{n}_2$ and therefore cannot generate interwell particle transport.

The most precise definition of the interwell current is through the Heisenberg equation for the number difference $\Delta\hat{N} = \hat{n}_1 - \hat{n}_2$:

$$\frac{d\Delta\hat{N}}{dt} = \frac{i}{\hbar}[\hat{H}, \Delta\hat{N}] = \frac{i}{\hbar}[\hat{H}_J, \Delta\hat{N}], \tag{106}$$

since $[\hat{H}_{\text{int}}, \Delta\hat{N}] = 0$.

We now compute $[\hat{H}_J, \Delta\hat{N}]$ explicitly. Using the commutators

$$[\hat{n}_1, \hat{a}_1^\dagger] = \hat{a}_1^\dagger, \qquad [\hat{n}_1, \hat{a}_1] = -\hat{a}_1, \qquad [\hat{n}_1, \hat{a}_2] = [\hat{n}_1, \hat{a}_2^\dagger] = 0, \tag{107}$$

we find

$$[\hat{n}_1, \hat{a}_1^\dagger \hat{a}_2] = \hat{a}_1^\dagger \hat{a}_2, \qquad [\hat{n}_2, \hat{a}_1^\dagger \hat{a}_2] = -\hat{a}_1^\dagger \hat{a}_2, \tag{108}$$

hence

$$[\Delta\hat{N}, \hat{a}_1^\dagger \hat{a}_2] = 2\hat{a}_1^\dagger \hat{a}_2 \qquad \Longrightarrow \qquad [\hat{a}_1^\dagger \hat{a}_2, \Delta\hat{N}] = -2\hat{a}_1^\dagger \hat{a}_2. \tag{109}$$

Similarly,

$$[\hat{a}_2^\dagger \hat{a}_1, \Delta\hat{N}] = +2\hat{a}_2^\dagger \hat{a}_1. \tag{110}$$

Therefore,

$$[\hat{H}_J, \Delta\hat{N}] = -J\left([\hat{a}_1^\dagger \hat{a}_2, \Delta\hat{N}] + [\hat{a}_2^\dagger \hat{a}_1, \Delta\hat{N}]\right) = 2J(\hat{a}_1^\dagger \hat{a}_2 - \hat{a}_2^\dagger \hat{a}_1). \tag{111}$$

Plugging into the Heisenberg equation,

$$\frac{d\Delta\hat{N}}{dt} = \frac{i}{\hbar} 2J(\hat{a}_1^\dagger \hat{a}_2 - \hat{a}_2^\dagger \hat{a}_1) = -\frac{2J}{\hbar}\,\hat{I}, \tag{112}$$

where we define the (dimensionless) current operator

$$\hat{I} \equiv -i(\hat{a}_1^\dagger \hat{a}_2 - \hat{a}_2^\dagger \hat{a}_1) = 2\hat{S}_y. \tag{113}$$

Equation (112) is the precise statement that the current is the generator of changes in the number imbalance.

6.2 From operators to classical Josephson equations and the pendulum dynamics

In the mean-field state, we have

$$\langle \hat{a}_1^\dagger \hat{a}_2 \rangle = \frac{N}{2} \sin\alpha\, e^{i\theta}, \qquad \langle \hat{I} \rangle = -i\left(\langle \hat{a}_1^\dagger \hat{a}_2 \rangle - \langle \hat{a}_2^\dagger \hat{a}_1 \rangle\right) = N \sin\alpha\, \sin\theta. \tag{114}$$

Taking expectation of (112) gives

$$\frac{d\langle \Delta\hat{N} \rangle}{dt} = -\frac{2J}{\hbar}\langle \hat{I} \rangle = -\frac{2J}{\hbar} N \sin\alpha\, \sin\theta. \tag{115}$$

At this point it is important to note that α is not an independent constant: it parameterizes the population imbalance,

$$\langle \Delta\hat{N} \rangle = N \cos\alpha, \tag{116}$$

so whenever particles flow and $\langle \Delta\hat{N} \rangle(t)$ changes, $\alpha(t)$ changes accordingly. Nevertheless, in the Josephson (small-oscillation) regime near the balanced configuration $\alpha \simeq \pi/2$, the variation of $\sin\alpha$ is a higher-order effect: writing $\alpha = \pi/2 + \delta\alpha$ with $|\delta\alpha| \ll 1$, one has

$$\sin\alpha = \cos(\delta\alpha) \approx 1 - \frac{\delta\alpha^2}{2}, \qquad \langle \Delta\hat{N} \rangle = N\cos\alpha \approx -N\,\delta\alpha, \tag{117}$$

so $\sin\alpha$ deviates from 1 only at order $(\Delta N/N)^2$. It is therefore consistent to approximate $\sin\alpha$ as a constant in this regime and introduce the Josephson energy scale

$$E_J \equiv 2JN\sin\alpha \approx \text{constant}, \tag{118}$$

so that

$$\frac{d\langle \Delta\hat{N} \rangle}{dt} = -\frac{E_J}{\hbar}\sin\theta. \tag{119}$$

The complementary equation for θ can be motivated as follows. In a weak-tunneling regime, the phase evolution in each well is dominated by the local interaction energy. For a number state $|N_i\rangle$ in well i, the interaction energy is $\frac{U}{2}N_i(N_i-1)$, hence the phase factor evolves as $e^{-i\frac{U}{2}N_i(N_i-1)t/\hbar}$. The relative phase thus accumulates at a rate proportional to the difference in interaction energies, which is proportional to ΔN for small deviations. This motivates

$$\frac{d\theta}{dt} = \frac{E_c}{\hbar}\langle \Delta\hat{N} \rangle, \tag{120}$$

where E_c is an effective "charging energy" scale proportional to U (its precise coefficient depends on conventions and on the regime of validity of the approximation).

A solid derivation of $\dot{\theta}$: A method based on TDVP

The Josephson equations are most cleanly understood as the *semiclassical* dynamics of the two-mode Bose–Hubbard model on the manifold of fixed-N mean-field states, i.e. SU(2) coherent states. This is the appropriate starting point whenever the system retains *first-order coherence* across the wells, $\langle \hat{a}_1^\dagger \hat{a}_2 \rangle = O(N)$, so that a relative phase is a meaningful collective variable. In the following, we would apply the celebrated *Time-Dependent Variational Principle* to systematically extract dynamical equations. For more details of TDVP, refer to the appendix.

(1) Variational principle and the effective action. We consider the time-dependent variational ansatz

$$|\Psi(\alpha,\theta)\rangle = \frac{1}{\sqrt{N!}}\left(\cos\frac{\alpha}{2}e^{-i\theta/2}\hat{a}_1^\dagger + \sin\frac{\alpha}{2}e^{i\theta/2}\hat{a}_2^\dagger\right)^N |0\rangle. \tag{121}$$

The time-dependent variational principle (TDVP) extremizes the action

$$\mathcal{S}_{\text{eff}} = \int dt \left[i\hbar\langle\Psi|\partial_t\Psi\rangle - \langle\Psi|\hat{H}|\Psi\rangle \right]. \tag{122}$$

Because the state is a condensate of N identical bosons in the same single-particle orbital, the Berry term is N times the single-particle Berry term:

$$i\hbar\langle\Psi|\partial_t\Psi\rangle = N\,i\hbar\langle\varphi|\partial_t\varphi\rangle, \qquad |\varphi\rangle = \cos\frac{\alpha}{2}e^{-i\theta/2}|1\rangle + \sin\frac{\alpha}{2}e^{i\theta/2}|2\rangle. \tag{123}$$

A direct differentiation gives

$$i\hbar\langle\varphi|\partial_t\varphi\rangle = \frac{\hbar}{2}\cos\alpha\,\dot{\theta}, \qquad \Rightarrow \qquad i\hbar\langle\Psi|\partial_t\Psi\rangle = \hbar\frac{N}{2}\cos\alpha\,\dot{\theta} = \hbar\frac{\Delta N}{2}\,\dot{\theta}, \tag{124}$$

where $\Delta N \equiv \langle \Delta\hat{N} \rangle = N \cos\alpha$. Equation (124) is the *origin* of the canonical structure: the relative phase θ is conjugate to the half-imbalance $\Delta N/2$.
(2) Mean-field energy and the classical Hamiltonian. Evaluating $\langle \Psi | \hat{H} | \Psi \rangle$ yields

$$\mathcal{E}(\alpha, \theta) = -JN \sin\alpha \cos\theta + \frac{UN^2}{4} \cos^2\alpha + \text{const.} \tag{125}$$

Using $\Delta N = N \cos\alpha$ and $N \sin\alpha = \sqrt{N^2 - (\Delta N)^2}$, we may write the classical Hamiltonian in the variables $(\Delta N, \theta)$ as

$$\mathcal{E}(\Delta N, \theta) = -J \sqrt{N^2 - (\Delta N)^2} \cos\theta + \frac{U}{4} (\Delta N)^2 + \text{const.} \tag{126}$$

(3) Equations of motion and the Josephson relations. From (124) the effective Lagrangian is

$$\mathcal{L}_{\text{eff}} = \hbar \frac{\Delta N}{2} \dot{\theta} - \mathcal{E}(\Delta N, \theta). \tag{127}$$

Varying $\mathcal{L}_{\text{eff}}$ gives Hamilton equations with canonical pair $(\theta, \Delta N/2)$:

$$\Delta\dot{N} = -\frac{2}{\hbar} \frac{\partial \mathcal{E}}{\partial \theta}, \qquad \dot{\theta} = \frac{2}{\hbar} \frac{\partial \mathcal{E}}{\partial (\Delta N)}. \tag{128}$$

Applying (128) to (126) yields the *nonlinear* Josephson equations

$$\Delta\dot{N} = -\frac{2J}{\hbar} \sqrt{N^2 - (\Delta N)^2} \sin\theta, \tag{129}$$

$$\dot{\theta} = \frac{U}{\hbar} \Delta N + \frac{2J}{\hbar} \frac{\Delta N}{\sqrt{N^2 - (\Delta N)^2}} \cos\theta. \tag{130}$$

In the Josephson (small-oscillation) regime $|\Delta N| \ll N$ and $|\theta| \ll 1$, one may expand

$$\sqrt{N^2 - (\Delta N)^2} \approx N, \qquad \frac{\Delta N}{\sqrt{N^2 - (\Delta N)^2}} \approx \frac{\Delta N}{N}, \tag{131}$$

so (130) reduces to

$$\dot{\theta} \approx \frac{1}{\hbar} \Big(U + \frac{2J}{N} \Big) \Delta N. \tag{132}$$

This identifies the "charging" scale in this convention (with $\Delta N = N_1 - N_2$) as

$$E_c \approx U + \frac{2J}{N} \simeq U \qquad (N \gg 1), \tag{133}$$

recovering the commonly used linearized relation $\dot{\theta} = (E_c/\hbar)\Delta N$. The correction $2J/N$ is the controlled contribution from the ΔN-dependence of the tunneling energy.

In practice we take the mean-field expectation values, $\Delta N \to \langle \Delta\hat{N} \rangle$, to obtain the closed Josephson equations (119) and (120).

Combining (119) and (120) yields

$$\frac{d^2\theta}{dt^2} = -\frac{E_c E_J}{\hbar^2} \sin\theta, \tag{134}$$

the equation of motion of a simple pendulum.

For small oscillations $|\theta| \ll 1$, $\sin\theta \simeq \theta$, giving a harmonic oscillation frequency

$$\omega_J = \frac{\sqrt{E_c E_J}}{\hbar}. \tag{135}$$

This regime exhibits Josephson oscillations in $\theta(t)$, $\Delta N(t)$, and the current.

For sufficiently large initial imbalance $\langle \Delta\hat{N}\rangle_0$ such that θ evolves rapidly, the current term $\sin\theta$ averages to (approximately) zero over time, leading to an approximately constant $\langle \Delta\hat{N}\rangle \simeq \langle \Delta\hat{N}\rangle_0$. This is the self-trapping regime.

7 Quantum Measurement and Interference: Ensemble Average vs Single-Shot Outcomes

7.1 Time-of-flight density and the absence of interference in ensemble averages for a Fock state

After releasing the double-well trap, the two initial localized modes evolve into expanding wavefunctions $\Psi_1(\boldsymbol{r}, t)$ and $\Psi_2(\boldsymbol{r}, t)$. In the two-mode approximation during expansion,

$$\hat{\Psi}(\boldsymbol{r}, t) = \Psi_1(\boldsymbol{r}, t)\hat{a}_1 + \Psi_2(\boldsymbol{r}, t)\hat{a}_2. \tag{136}$$

The ensemble-averaged density is

$$n(\boldsymbol{r}, t) = \langle \hat{\Psi}^\dagger(\boldsymbol{r}, t)\hat{\Psi}(\boldsymbol{r}, t)\rangle = \sum_{i=1}^{2} \langle \hat{n}_i\rangle |\Psi_i(\boldsymbol{r}, t)|^2 + \Psi_1^*(\boldsymbol{r}, t)\Psi_2(\boldsymbol{r}, t)\langle \hat{a}_1^\dagger \hat{a}_2\rangle + \Psi_2^*(\boldsymbol{r}, t)\Psi_1(\boldsymbol{r}, t)\langle \hat{a}_2^\dagger \hat{a}_1\rangle. \tag{137}$$

For the repulsive strong-interaction Fock state $|N/2, N/2\rangle$, one has $\langle \hat{a}_1^\dagger \hat{a}_2\rangle = 0$. Therefore,

$$n(\boldsymbol{r}, t) = \langle \hat{n}_1\rangle |\Psi_1(\boldsymbol{r}, t)|^2 + \langle \hat{n}_2\rangle |\Psi_2(\boldsymbol{r}, t)|^2, \tag{138}$$

which contains no interference term. Thus interference fringes are absent in the ensemble-averaged density for an initially phase-incoherent Fock state.

7.2 Why single shots show fringes: phase localization by measurement (projection picture)

Despite the ensemble-average result, experiments show interference fringes in each individual run, with a random relative phase that varies from shot to shot. This is a measurement effect: the measurement does not merely reveal a pre-existing relative phase; it *projects* the many-body state into a state with a definite phase.

A key identity is that a number-squeezed state can be represented as a superposition over relative phases. In particular, for even N, one may express the balanced Fock state as

$$\left|\frac{N}{2}, \frac{N}{2}\right\rangle \propto \int_{-\pi}^{\pi} d\theta \left(\frac{\hat{a}_1^\dagger e^{i\theta/2} + \hat{a}_2^\dagger e^{-i\theta/2}}{\sqrt{2}}\right)^N |0\rangle, \tag{139}$$

which is a continuous superposition of simple condensates with all possible relative phases θ. The integral representation can be verified by expanding the integrand in powers of $\hat{a}_1^\dagger$ and $\hat{a}_2^\dagger$: only the term with equal powers survives the θ-integral due to

$$\int_{-\pi}^{\pi} d\theta\, e^{im\theta} = 2\pi\,\delta_{m,0} \quad \text{for integer } m, \tag{140}$$

which projects out the $N_1 = N_2$ component.

In a time-of-flight measurement, detecting an atom at position $\boldsymbol{r}$ is modeled (at the level of state update) by applying the field operator $\hat{\Psi}(\boldsymbol{r}, t)$ to the pre-measurement state. Since

$$\hat{\Psi}(\boldsymbol{r}, t) \propto \Psi_1(\boldsymbol{r}, t)\hat{a}_1 + \Psi_2(\boldsymbol{r}, t)\hat{a}_2, \tag{141}$$

each detection applies a superposition of $\hat{a}_1$ and $\hat{a}_2$, with a relative complex phase determined by the ratio $\Psi_2(\boldsymbol{r}, t)/\Psi_1(\boldsymbol{r}, t)$. Successive detections therefore update the conditional state in a way that rapidly *sharpens* the distribution over θ in (139). The outcome is that, within a single experimental run, the conditional many-body state becomes well-approximated by a simple condensate with a definite (but random) relative phase; consequently, the observed density profile in that run exhibits clear fringes. Across many runs, the selected phase is random, and the fringes wash out upon averaging, consistent with the ensemble result.

8 Hanbury–Brown–Twiss (HBT) Effect: Interference in Density–Density Correlations

8.1 Second-order correlation function and the exchange interference term

Even when the first-order coherence $\langle \hat{a}_1^\dagger \hat{a}_2 \rangle$ vanishes, interference can persist in *second-order* correlations due to bosonic exchange.

Consider the density–density correlator

$$G^{(2)}(\boldsymbol{r}, \boldsymbol{r}'; t) \equiv \left\langle \hat{\Psi}^\dagger(\boldsymbol{r}, t)\hat{\Psi}(\boldsymbol{r}, t)\hat{\Psi}^\dagger(\boldsymbol{r}', t)\hat{\Psi}(\boldsymbol{r}', t) \right\rangle. \tag{142}$$

Substitute $\hat{\Psi}(\boldsymbol{r}, t) = \Psi_1(\boldsymbol{r}, t)\hat{a}_1 + \Psi_2(\boldsymbol{r}, t)\hat{a}_2$. Expanding and using that for an initial Fock state with no first-order coherence $\langle \hat{a}_1^\dagger \hat{a}_2 \rangle = 0$, one finds a general structure

$$G^{(2)}(\boldsymbol{r}, \boldsymbol{r}'; t) = n(\boldsymbol{r}, t)n(\boldsymbol{r}', t) + \langle \hat{n}_1 \rangle \langle \hat{n}_2 \rangle \left(\Psi_1^*(\boldsymbol{r}, t)\Psi_2^*(\boldsymbol{r}', t)\Psi_2(\boldsymbol{r}, t)\Psi_1(\boldsymbol{r}', t) + \text{h.c.} \right), \tag{143}$$

where $n(\boldsymbol{r}, t)$ is the ensemble-averaged density computed previously. The second term in (143) is the HBT exchange term: it oscillates spatially whenever the expanding wavefunctions overlap, producing interference peaks in the noise correlations even though the average density shows no fringes.

This mechanism underlies the observation of interference peaks in time-of-flight noise correlations of bosons released from a Mott insulator: the Mott state lacks phase coherence between sites, but the density–density correlations reveal the underlying lattice structure through exchange interference.

9 Attractive Interaction: Schrödinger Cat States and Spontaneous Symmetry Breaking

9.1 Mean-field symmetry breaking vs the uniqueness of the exact ground state

For $U < 0$ and sufficiently strong attraction $|U|N \gtrsim 2J$, mean-field theory predicts two degenerate minima corresponding to macroscopic localization in either well, apparently breaking the left-right exchange symmetry $\hat{a}_1 \leftrightarrow \hat{a}_2$ (a Z_2 symmetry).

However, in the exact quantum problem at finite N, the ground state of a real Hamiltonian in a connected Hilbert space is typically unique and can be chosen to respect all symmetries. The resolution is that the exact ground state remains symmetric but becomes a coherent superposition of two macroscopically distinct configurations, while the energy splitting to the first antisymmetric state becomes extremely small as N grows, making symmetry breaking effectively stable in practice.

9.2 Exact cat (NOON) states in the strong-attraction limit and their diagnostics

In the strong-attraction limit $U \to -\infty$, the two lowest-energy classical configurations are $|N,0\rangle$ and $|0,N\rangle$. The symmetric and antisymmetric superpositions are

$$|\Psi_+\rangle = \frac{1}{\sqrt{2}}\left(|N,0\rangle + |0,N\rangle\right), \qquad |\Psi_-\rangle = \frac{1}{\sqrt{2}}\left(|N,0\rangle - |0,N\rangle\right). \tag{144}$$

The symmetric state $|\Psi_+\rangle$ is the ground state and is known as a NOON state; it is a paradigmatic Schrödinger cat state because its two components are macroscopically distinct.

The one-body density matrix of $|\Psi_+\rangle$ is

$$\rho^{(1)} = \frac{N}{2}\begin{pmatrix} 1 & 0 \\ 0 & 1 \end{pmatrix}, \tag{145}$$

the same as that of the repulsive Fock state $|N/2, N/2\rangle$. Hence by the one-body criterion, the cat state is also fragmented.

Nevertheless, the number-imbalance fluctuations are drastically different. For $|\Psi_+\rangle$,

$$\Delta\hat{N}|N,0\rangle = N|N,0\rangle, \qquad \Delta\hat{N}|0,N\rangle = -N|0,N\rangle, \tag{146}$$

so

$$\langle\Psi_+|(\Delta\hat{N})^2|\Psi_+\rangle = N^2, \tag{147}$$

i.e. $\langle(\Delta\hat{N})^2\rangle \propto N^2$, reflecting macroscopic superposition. This contrasts with the repulsive Fock state, where $\langle(\Delta\hat{N})^2\rangle = 0$. Moreover, the two states differ at the level of higher-order density matrices: the repulsive Fock state can be viewed as a pair condensate in the two-body sector, while the NOON cat state cannot be interpreted as condensation of pairs in the same sense.

9.3 Macroscopic quantum tunneling and the exponentially small splitting

Why are cat states rare and fragile in nature? The crucial point is that the coupling between macroscopically distinct states is generated by *many* local steps. In the double-well model, the tunneling Hamiltonian moves only one particle at a time. To connect $|N,0\rangle$ and $|0,N\rangle$ one must traverse a sequence of intermediate states:

$$|N,0\rangle \to |N-1,1\rangle \to |N-2,2\rangle \to \cdots \to |1,N-1\rangle \to |0,N\rangle, \tag{148}$$

which involves N single-particle tunneling events and incurs increasing interaction-energy costs along the path. This multi-step process is called *macroscopic quantum tunneling*.

A quantitative way to see the suppression is to treat $\hat{H}_J$ as a perturbation in the limit $|U| \gg J$. The unperturbed energies (up to an irrelevant constant) are

$$E_0(N_1) = \frac{U}{2}\left[N_1(N_1-1) + (N-N_1)(N-N_1-1)\right]. \tag{149}$$

The states $|N,0\rangle$ and $|0,N\rangle$ are degenerate at this level. The effective coupling between them appears only at N-th order in J, because each application of $\hat{H}_J$ changes N_1 by ± 1. The resulting effective two-level Hamiltonian in the $\{|N,0\rangle, |0,N\rangle\}$ subspace has an off-diagonal matrix element t_{eff} of the schematic form

$$t_{\text{eff}} \sim (-J)^N \prod_{k=1}^{N-1} \frac{\sqrt{(N-k+1)k}\,\sqrt{(N-k)(k+1)}}{E_0(N-k) - E_0(N)}, \tag{150}$$

where the denominators are the interaction-energy penalties of intermediate states with populations $(N-k, k)$. The key point is that the denominators grow with N and with $k(N-k)$,

while the numerator grows at most factorially; the net result is that t_{eff} (and hence the energy splitting $E_- - E_+ \sim 2|t_{\text{eff}}|$) decreases extremely rapidly with N, effectively exponentially in N for fixed $J/|U|$.

Thus the symmetric and antisymmetric cat states become nearly degenerate for surprisingly small N, making the system extraordinarily sensitive to any symmetry-breaking perturbation.

9.4 Why spontaneous symmetry breaking is stable: infinitesimal bias and astronomically long tunneling times

Because the splitting between $|\Psi_+\rangle$ and $|\Psi_-\rangle$ is so small, an infinitesimal left-right bias term,

$$\hat{H}_\epsilon = \epsilon(\hat{n}_1 - \hat{n}_2) = \epsilon\,\Delta\hat{N}, \tag{151}$$

produces an energy difference between $|N,0\rangle$ and $|0,N\rangle$ of magnitude

$$\Delta E_\epsilon = \epsilon N. \tag{152}$$

For large N, ϵN easily overwhelms the exponentially small t_{eff}, so the true ground state becomes essentially $|N,0\rangle$ or $|0,N\rangle$, i.e. a symmetry-breaking state.

A complementary dynamical viewpoint is the following. Suppose the system is prepared in a symmetry-breaking configuration due to a tiny bias. If the bias is then removed so that the Hamiltonian regains exact Z_2 symmetry, the system could in principle tunnel between the two macroscopic configurations and restore symmetry in time. However, the tunneling timescale is set by the inverse splitting,

$$\tau_{\text{tunnel}} \sim \frac{\hbar}{E_- - E_+} \sim \frac{\hbar}{2|t_{\text{eff}}|}, \tag{153}$$

which becomes astronomically large as N grows. Therefore, on any realistic timescale, the system remains trapped in one symmetry-breaking sector. This is the operational content of spontaneous symmetry breaking in large many-body systems: the symmetric cat state is the exact eigenstate in principle, but it is unobservable in practice due to extreme fragility and timescale separation.

> The fragility of Schrödinger cat states and the stability of spontaneous symmetry breaking are two sides of the same mechanism: **local** Hamiltonian terms couple macroscopically distinct configurations only through **macroscopically many** virtual steps, making the effective coupling (and the symmetric–antisymmetric splitting) extremely small at large system size.

10 Summary: Regimes of the Bosonic Double-Well Model and the Core Physical Picture

10.1 Regime map: ground states, coherence, and dynamics

The bosonic double-well (two-mode Bose–Hubbard) Hamiltonian

$$\hat{H} = -J(\hat{a}_1^\dagger \hat{a}_2 + \hat{a}_2^\dagger \hat{a}_1) + \frac{U}{2}\Big[\hat{n}_1(\hat{n}_1 - 1) + \hat{n}_2(\hat{n}_2 - 1)\Big] \tag{154}$$

exhibits distinct behaviors depending on the sign and magnitude of U relative to J and on the particle number N. The most transparent organizing principles are (i) whether the ground state carries *first-order phase coherence* across the wells, and (ii) whether the low-energy dynamics is

governed by Josephson-type coupled motion of number imbalance and relative phase.

■ **Noninteracting and weakly repulsive regime**

Simple condensate with robust phase coherence ($U \geq 0$, $UN/J \ll 1$ or moderate)

For $U = 0$, the single-particle tunneling term is minimized by the symmetric orbital $\hat{b}_g^\dagger = (\hat{a}_1^\dagger + \hat{a}_2^\dagger)/\sqrt{2}$, and the many-body ground state places all N bosons in this lowest orbital,

$$|\Psi_0\rangle = \frac{1}{\sqrt{N!}}(\hat{b}_g^\dagger)^N|0\rangle. \tag{155}$$

This is a *simple condensate*: the one-body density matrix has one eigenvalue of order N and the other is $O(1)$. For repulsive $U > 0$ that is not too strong, the ground state remains close to a single condensate with appreciable off-diagonal coherence $\langle \hat{a}_1^\dagger \hat{a}_2 \rangle = O(N)$, while number fluctuations are only weakly squeezed compared with the $U = 0$ binomial/Gaussian distribution $\langle (\Delta \hat{N})^2 \rangle \sim N$.

■ **Strongly repulsive regime**

Number-squeezed / Fock-like limit and fragmentation ($U > 0$, $JN/U \ll 1$)

As U increases, the competition between tunneling (favoring coherence) and interactions (penalizing imbalance fluctuations) squeezes the distribution of Fock components Ψ_l in the basis $|N/2 + l, N/2 - l\rangle$. In the large-N harmonic approximation to the discrete Schrödinger equation in l, the ground-state envelope remains Gaussian but its width is strongly reduced,

$$\Psi_l \propto e^{-l^2/\sigma_{\Delta N}^2}, \qquad \langle (\Delta \hat{N})^2 \rangle \sim \sigma_{\Delta N}^2 \propto \sqrt{\frac{JN}{U}}. \tag{156}$$

In the extreme limit $JN/U \ll 1$, the ground state approaches the Fock state with fixed populations,

$$|\Psi\rangle \to \frac{\hat{a}_1^{\dagger N/2} \hat{a}_2^{\dagger N/2}}{(N/2)!}|0\rangle, \tag{157}$$

for which $\langle \hat{a}_1^\dagger \hat{a}_2 \rangle \to 0$ and the one-body density matrix has two macroscopic eigenvalues $\sim N/2$, i.e. the condensate is *fragmented* in the one-body sense. In this regime, phase coherence is lost (large phase fluctuations) while number imbalance fluctuations are suppressed.

■ **Attractive regime**

Mean-field symmetry breaking versus exact cat ground states ($U < 0$)

For $U < 0$, mean-field theory predicts a transition when $|U|N$ exceeds $2J$: the energy landscape develops two degenerate minima corresponding to macroscopic occupation of either well, i.e. states that break the Z_2 exchange symmetry. The exact finite-N solution of the symmetric Hamiltonian, however, has a unique ground state that respects Z_2 and becomes a Schrödinger-cat (NOON) state in the strong-attraction limit,

$$|\Psi_+\rangle \to \frac{1}{\sqrt{2}}\Big(|N, 0\rangle + |0, N\rangle\Big), \tag{158}$$

with a nearly-degenerate first excited partner

$$|\Psi_-\rangle \to \frac{1}{\sqrt{2}}\Big(|N, 0\rangle - |0, N\rangle\Big). \tag{159}$$

The splitting between these two states is exponentially small in N, reflecting *macroscopic quantum tunneling* that requires $O(N)$ successive single-particle tunneling events through high-energy intermediate configurations. Consequently, infinitesimal asymmetries $\epsilon(\hat{n}_1 - \hat{n}_2)$ generically pin the system into a symmetry-broken configuration $|N, 0\rangle$ or $|0, N\rangle$, explaining why robust macroscopic cat states are rare in nature and why symmetry breaking becomes effectively stable for large N.

■ **Josephson dynamics**

Coupled oscillations versus self-trapping (typically $U > 0$, with non-equilibrium initial conditions)

In coherent regimes the relevant slow collective variables are the number imbalance ΔN and the relative phase θ. The current operator is generated solely by the tunneling term and satisfies

$$\frac{d\Delta\hat{N}}{dt} = -\frac{2J}{\hbar}\hat{I}, \qquad \hat{I} = -i(\hat{a}_1^\dagger \hat{a}_2 - \hat{a}_2^\dagger \hat{a}_1). \tag{160}$$

Within the Josephson regime (small excursions near balance), one obtains the coupled Josephson equations

$$\frac{d\langle\Delta\hat{N}\rangle}{dt} = -\frac{E_J}{\hbar}\sin\theta, \qquad \frac{d\theta}{dt} = \frac{E_c}{\hbar}\langle\Delta\hat{N}\rangle, \tag{161}$$

leading to a pendulum equation for θ and a small-oscillation frequency $\omega_J = \sqrt{E_J E_c}/\hbar$. For sufficiently small initial imbalance and phase, the system exhibits Josephson oscillations; for sufficiently large initial imbalance (relative to the scale set by E_J/E_c), the dynamics crosses over to a self-trapping regime in which $\langle\Delta\hat{N}\rangle$ remains close to its initial value while θ runs approximately linearly in time.

■ **Interference, measurement, and HBT correlations: coherence "created" by measurement**

A number-squeezed (Fock-like) initial state has $\langle\hat{a}_1^\dagger\hat{a}_2\rangle = 0$, so the ensemble-averaged density after release is simply the incoherent sum of the two expanding clouds and shows no interference fringes. Nevertheless, in a single experimental run one typically observes interference: the measurement of identical bosons effectively projects the initial state onto a state with a definite relative phase, which is random from shot to shot, so fringes wash out under averaging. Even after ensemble averaging, the density–density correlator can exhibit interference peaks (Hanbury–Brown–Twiss effect), reflecting exchange symmetry of identical bosons rather than a pre-existing first-order phase coherence.

10.2 Core physical picture of the note: a collective "pseudo-spin" and the number–phase complementarity

The central unifying picture is that a two-mode bosonic system is a single collective object with an emergent $\mathfrak{su}(2)$ algebra (Schwinger bosons). Fixing the total particle number N fixes the collective spin length $S = N/2$, and the low-energy physics is governed by how this collective spin is oriented and fluctuates on the Bloch sphere. Tunneling J acts as an effective transverse field $-2J\hat{S}_x$ favoring phase coherence (alignment in the x direction), while Interactions U act as an "easy-axis" anisotropy $U\hat{S}_z^2$ favoring number squeezing (localization in S_z).

In the coherent regime the state is well-approximated by an SU(2) coherent state with a well-defined relative phase and large number fluctuations; in the strongly repulsive regime number fluctuations are suppressed and phase fluctuates strongly, producing fragmentation and loss of first-order coherence. The Josephson effect is the dynamical counterpart of this structure: ΔN and θ form an (approximately) conjugate pair, so the tunneling term generates a current that changes ΔN, while interactions generate a phase evolution sensitive to ΔN. For

attractive interactions, the same collective structure explains the appearance of macroscopic superpositions (cat states) in the exact symmetric problem and their fragility under infinitesimal symmetry-breaking perturbations, clarifying the many-body origin of spontaneous symmetry breaking as the large-N limit of exponentially small tunneling between macroscopically distinct configurations.

A Time-Dependent Variational Principle (TDVP)

Key Idea: projecting quantum dynamics onto a variational manifold

The time-dependent variational principle (TDVP) provides a systematic way to approximate the Schrödinger dynamics by restricting the state to a chosen family of trial states. Suppose we select a variational manifold (a parameterized family)

$$\mathcal{M} = \left\{ |\psi(\boldsymbol{\lambda})\rangle \,\middle|\, \boldsymbol{\lambda} = (\lambda^1, \ldots, \lambda^d) \in \mathbb{C}^d \right\}, \tag{162}$$

and we only allow the wave function to evolve *within* $\mathcal{M}$, i.e. $|\psi(t)\rangle = |\psi(\boldsymbol{\lambda}(t))\rangle$. TDVP then prescribes a "best" trajectory $\boldsymbol{\lambda}(t)$ by enforcing self-consistency with the exact equation of motion in an optimal (projection) sense.

(1) Action formulation. A convenient and widely used formulation is to extremize the Dirac–Frenkel action restricted to $\mathcal{M}$,

$$\mathcal{S}_{\mathrm{TDVP}}[\boldsymbol{\lambda}] = \int dt \left[i\hbar \langle \psi(\boldsymbol{\lambda}) | \partial_t \psi(\boldsymbol{\lambda}) \rangle - \langle \psi(\boldsymbol{\lambda}) | \hat{H} | \psi(\boldsymbol{\lambda}) \rangle \right]. \tag{163}$$

The first term is a Berry-phase term; geometrically it endows $\mathcal{M}$ with an induced symplectic (or more generally Kähler) structure, while the second term is the energy functional

$$\mathcal{E}(\boldsymbol{\lambda}) = \langle \psi(\boldsymbol{\lambda}) | \hat{H} | \psi(\boldsymbol{\lambda}) \rangle. \tag{164}$$

Varying (163) with respect to $\boldsymbol{\lambda}(t)$ yields coupled equations of motion for the variational parameters. In favorable coordinates (e.g. coherent-state manifolds), these take an explicit Hamilton form in terms of canonically conjugate variables, making the connection to semiclassical dynamics manifest.

(2) Projection formulation (Dirac–Frenkel condition). An equivalent statement is that the TDVP trajectory makes the residual vector

$$|\mathcal{R}\rangle \equiv i\hbar\, \partial_t |\psi(\boldsymbol{\lambda})\rangle - \hat{H} |\psi(\boldsymbol{\lambda})\rangle \tag{165}$$

orthogonal to the tangent space of the manifold at each time. Concretely, for any tangent vector $|\delta\psi\rangle \in T_{|\psi\rangle}\mathcal{M}$,

$$\langle \delta\psi | \mathcal{R} \rangle = 0. \tag{166}$$

Intuitively, this means that the exact quantum "velocity" $-\frac{i}{\hbar}\hat{H}|\psi\rangle$ is projected onto the accessible directions $\partial_{\lambda^a}|\psi\rangle$, so the evolution is the most faithful possible within the restricted ansatz class.

(3) Why TDVP is powerful in many-body physics. The choice of $\mathcal{M}$ is physics-driven. If $\mathcal{M}$ captures the relevant correlations and symmetries, TDVP yields controlled effective dynamics, often with a clear large-parameter expansion (e.g. $1/N$ for coherent states or semiclassical limits). In the bosonic double-well problem, taking $\mathcal{M}$ to be the fixed-N SU(2) coherent states produces an effective action whose Berry term is $\hbar(\Delta N/2)\dot{\theta}$, thereby deriving the canonical structure and the Josephson equations in a conceptually clean way.

(4) Modern numerical applications. Beyond analytic semiclassical reductions, TDVP is a central tool in contemporary real-time and imaginary-time simulations of correlated quantum

systems. A prominent example is *MPS-TDVP*: one restricts $\mathcal{M}$ to the manifold of matrix product states (MPS) with a fixed bond dimension χ, and applies (166) to obtain an evolution that stays within the MPS manifold. This provides a robust alternative to Trotterized time evolution, typically improving the stability of long-time dynamics and offering a principled way to control truncation errors by increasing χ. Analogous TDVP schemes exist for other tensor-network manifolds (e.g. tree tensor networks and PEPS in appropriate settings), as well as for variational quantum algorithms where parameters are updated by projecting dynamics onto a circuit ansatz.